ELSEVIER

Coordination Chemistry Reviews 228 (2002) 115–126

COORDINATION CHEMISTRY REVIEWS

www.elsevier.com/locate/ccr

Synthesis, structures and properties of hydrolytic Al(III) aggregates and Fe(III) analogues formed with iminodiacetate-based chelating ligands

Wolfgang Schmitt [a], Peter A. Jordan [b], Richard K. Henderson [b], Geoffrey R. Moore [b], Christopher E. Anson [a], Annie K. Powell [a,*]

[a] *Institute for Inorganic Chemistry, University of Karlsruhe, Engesserstrasse Geb. 30.45, D-76128 Karlsruhe, Germany*
[b] *School of Chemical Sciences, University of East Anglia, Norwich NR4 7TJ, UK*

Received 14 August 2001; accepted 7 December 2001

Contents

Abstract

Both Al(III) and Fe(III) display a rich hydrolytic chemistry which can lead to the formation of a variety of aggregated oxo and hydroxo-bridged aggregates. The formation, structures and properties of these species are important in defining the availability and reactivity of these species in aqueous environments such as are found in biological systems and the environment. Although there are many similarities in the behaviour of the Al^{3+} and Fe^{3+} ions there are also some important differences between these two metal ions which can lead to a divergence in their chemistries. These considerations are discussed and illustrated with reference to 16 Al(III) and Fe(III) compounds, which have been crystallographically characterised, and which form in aqueous environments in the presence of chelating ligands containing the iminodiacetate functionality.

Keywords: Hydrolytic Al(III) aggregates; Fe(III) analogues; Iminodiacetate-based chelating ligands

* Corresponding author.
E-mail address: powell@achpc50.chemie.uni-karlsruhe.de (A.K. Powell).

0010-8545/02/$ - see front matter
PII: S0010-8545(02)00110-8

1. Introduction

A key feature in the transition of aluminium(III) from the geological chemistry of the Earth, its common habitat, to the biological chemistry of living systems, where it is non-essential, is the formation of soluble aluminium(III)–ligand complexes. Such complexes, which form in aqueous environments, allow aluminium to become bioavailable and govern the metabolism of Al(III). This defines the distribution, storage, possible toxic effects and clearance of the metal. Also of importance is the interaction of the small and highly charged Al^{3+} ion with water itself. The aqueous chemistry of Al(III) is strongly influenced by hydrolytic processes in much the same way as observed for the similar Fe^{3+} (h.s.) ion. In biochemical terms this similarity is important because whilst iron is an essential element to virtually all life forms, aluminium is not and is capable of disrupting biochemical processes [1]. It is possible that Al(III) is able to utilise iron-uptake pathways but thereafter the chemistry of the two ions is likely to diverge since iron takes part in extensive redox processes to fulfil its biochemical functions whereby it can interact with a variety of donor atom types depending on oxidation and spin state, whereas aluminium is redox inactive and thus will continue to participate in hydrolytically governed chemistry interacting with essentially hard donor atoms. It is therefore instructive to compare the aqueous coordination chemistry of Al(III) and Fe(III) in the presence of ligands which contain the sorts of hard donor groups which are likely to be important in natural systems. This should shed some light on the parallels and differences in behaviour of the two metal ions in terms of structural details and perhaps even relative reactivity. Here we compare the complexes we have isolated and structurally characterised using three ligands which contain the iminodiacetic acid functionality: iminodiacetic acid itself, H_2ida; hydroxyethyliminodiacetic acid, H_3heidi; and hydroxypropanediaminotetraacetic acid, H_5hpdta. The relationship of these to one another is shown in Fig. 1.

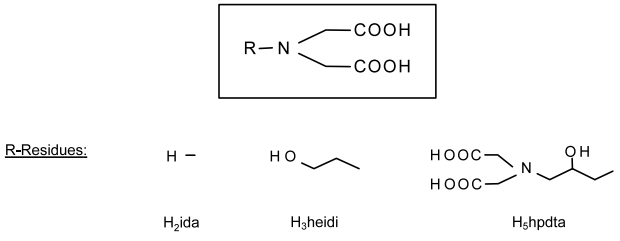

Fig. 1. Ligands used in these studies.

2. Experimental

The methods for the preparation of compounds **5**–**10**, and **16** and the details of their crystal structure analyses have been reported previously [3–5].

2.1. Synthesis

All chemicals were used as received from Aldrich Chemicals.

2.1.1. Preparation of $Na[Al(ida)_2]\cdot 1.5H_2O$ (**1**)

The product was formed by addition of a solution of 1.997 g H_2ida (15 mmol) and NaOH (20 mmol, 0.08 g) in distilled water (10 ml) to a solution of 0.935 g $Al(NO_3)_3\cdot 9H_2O$ 2.5 mmol) in distilled water (10 ml) giving an almost colourless solution of pH 5.5. Colourless crystals were formed after 1 week but were allowed to grow further to provide ones more suitable for X-ray diffraction.

Elemental analysis, calculated for $AlC_8H_{13}\cdot N_2NaO_{9.5}$: C, 28.3; H, 3.9; N, 8.3; found: C, 28.3; H, 3.8; N, 8.5%. IR data: 3560 cm^{-1} (s, br); 3240 cm^{-1} (ms); 1664 cm^{-1} (vs); 1384 cm^{-1} (ms); 1170 cm^{-1} (m).

2.1.2. Preparation of $K[Fe(ida)_2]\cdot 3H_2O$ (**2**)

$K[Fe(ida)_2]\cdot 3H_2O$ was formed by the addition of a solution of 0.99 g H_2ida (7.5 mmol) and 0.84 g KOH (15 mmol) in distilled water (10 ml) to a solution of $FeCl_3$ (2.5 mmol, 0.40 g) in 10 ml water giving a golden brown solution of pH 4. Green crystals were obtained from water/ethanol mixtures after 1 day. Yield: 0.65 g (63% based on $FeCl_3$).

Elemental analysis, calculated for $C_8FeH_{16}KN_2O_{11}$: C, 23.1; H, 3.7; N, 6.7; found: C, 23.1; H, 3.9; N, 6.8%. IR data: 3428 cm^{-1} (s, br); 3214 (s); 1661 cm^{-1} (vs); 1348 cm^{-1} (s); 1328 cm^{-1} (s); 625 cm^{-1} (m).

2.1.3. Preparation of $K_4[\{Fe(ida)_2\}_2O]\cdot 10H_2O$ (**3**)

Addition of a solution of 0.99 g H_2ida (7.5 mmol) and 0.84 g KOH (30 mmol) in distilled water (10 ml) to a solution of $FeCl_3$ (2.5 mmol, 0.40 g) in 10 ml water gave a brown solution of pH 8. Red crystals of were obtained from water/ethanol mixtures after 2 weeks. Yield: 0.61 g (49% based on of $FeCl_3$).

Elemental analysis, calculated for $C_{16}Fe_2H_{38}K_4N_4O_{26}$ which corresponds to the crystallographically determined formulation with the loss of one water molecule: C, 19.8; H, 4.0; N, 5.8; found: C, 20.3; H, 3.6; N, 5.8%. IR data: 3428 cm^{-1} (s, br); 3267 (s); 2930 cm^{-1} (w); 1616 cm^{-1} (vs); 1392 cm^{-1} (vs); 675 cm^{-1} (ms).

2.1.4. Preparation of $[Al(ida)(H_2O)(OH)]_2\cdot 2H_2O$ (**4**)

The product was formed by addition of 0.333 g H_2ida (2.5 mmol) and NaOH 0.40 g (5 mmol) in distilled water (10 ml) to 0.935g $Al(NO_3)_3\cdot 9H_2O$ (2.5 mmol) in distilled

water 10 ml) to give a clear solution of pH 3.3. The volume was then made up to approximately 100 ml with ethanol. Crystals suitable for diffraction were recovered after 2–3 weeks. Yield: 0.16 g (30% based on based on $Al(NO_3)_3 \cdot 9H_2O$). Elemental analysis, calculated for $AlC_4H_{10}NO_7$: C, 22.2; H, 4.7; N, 6.5; found: C, 22.8; H, 4.8; N, 6.8%. IR data: 3496 cm^{-1} (s, br); 3320 cm^{-1} (ms); 1680 cm^{-1} (vs); 1655 cm^{-1} (vs); 1390 cm^{-1} (ms).

2.1.5. Preparation of $[Fe_2(hpdta)(H_2O)_3Cl] \cdot 3H_2O$ (**11**)

0.081 g (2.5 mmol) H_5hpdta and 0.135 g (5 mmol) $FeCl_3 \cdot 6H_2O$ were dissolved in 5 ml distilled water by addition of 0.081 ml pyridine. Slow evaporation of the solvent gave orange hexagonal crystals after 7 days. X-ray studies revealed that this complex consists of a rectangular arrangement of four iron(III) centres with water ligands comparable to compound **12**. The reaction vessel was sealed. In the presence of chloride we observed the decomposition of the initial compound to form yellow–green crystals of the dinuclear compound within 8 weeks. Yield: 0.096 g (71% based on $FeCl_3 \cdot 6H_2O$).

Elemental analysis, calculated for $C_{11}ClFe_2H_{25}O_{15}N_2$: C, 23.08; H, 4.40; N, 4.89; found: C, 22.99; H, 4.61; N, 5.01%. IR data: 3391 cm^{-1} (s, br); 1641 (vs); 1633 cm^{-1} (vs); 1583 cm^{-1} (vs); 1371 cm^{-1} (s); 923 cm^{-1} (ms); 731 cm^{-1} (m); 600 cm^{-1} (m).

2.1.6. Preparation of $NH_4[Fe_4O(OH)(hpdta)_2(H_2O)_4]12 \cdot 5H_2O$ (**12**)

0.081 g (0. 25 mmol) H_5dpta was dissolved in 1 ml distilled water containing 1.3 ml ammonia solution (2 M). The ligand was then added to a solution of 1.25 ml of iron(III) nitrate nonahydrate (0.4 M). Addition of 1 ml dimethylacetamide as cosolvent and slow evaporation of the solvent led to the formation of orange red crystals of **12** after 5 days. Yield: 0.064 g (47% based on based on $Fe(NO_3)_3 \cdot 9H_2O$). Elemental analysis, calculated for $C_{22}Fe_4H_{53}N_5O_{31}$ which corresponds to the crystallographically determined formulation with the loss of 5.5 water molecules: C, 23.85; H, 4.83; N, 6.32; found: C, 23.74; H, 5.04; N, 6.47%. IR data: 3423 cm^{-1} (s, br); 3198 (sh); 1637 cm^{-1} (vs); 1384 cm^{-1} (vs); 919 cm^{-1} (m); 742 cm^{-1} (m); 606 cm^{-1} (m).

2.1.7. Preparation of $(enH_2)[Al_4(OH)_4(hpdta)_2] \cdot 7.5H_2O$ (**13**)

0.162 g (0.5 mmol) H_5hpdta and 0.120 g (0.5 mmol) $AlCl_3 \cdot 6H_2O$ were dissolved in 6 ml distilled water by dropwise addition of ethylenediamine to a pH value of 5.8. Slow evaporation of the solvent led to the formation of colourless hexagonal crystals. Yield: 0.023 g (18% based on $AlCl_3 \cdot 6H_2O$). IR data: 3434 cm^{-1} (s, br); 1666 cm^{-1} (vs); 1401 cm^{-1} (ms); 1173 cm^{-1} (m); 925 cm^{-1} (m); 759 cm^{-1} (ms). Elemental analysis, calculated for $Al_4C_{24}H_{49}N_6O_{26.5}$, corresponds to the crystallographically determined formulation with the loss of three water molecules: C, 30.74; H, 5.27; N, 8.96; found: C, 30.61; H, 5.44; N, 9.07%.

2.1.8. Preparation of $(enH_2)_{1.5}[Fe_4O(OH)_3(hpdta)_2] \cdot 6H_2O$ (**14**)

0.081 g (0.25 mmol) H_5hpdta and 0.202 g (0.5 mmol) $Fe(NO_3)_3 \cdot 9H_2O$ were dissolved in 6 ml distilled water by dropwise addition of ethylenediamine up to pH 7.0. Addition of 5 ml dimethylacetamide led to the formation of dark red rhombic crystals within 3 days. Yield: 0.101 g (71% based on $Fe(NO_3)_3 \cdot 9H_2O$).

Elemental analysis, calculated for $C_{25}Fe_4H_{54}N_7O_{28}$: C, 26.71; H, 4.85; N, 8.72; found: C, 26.64; H, 4.88; N, 8.58%. IR data: 3416 cm^{-1} (s, br); 2959 (s); 2950 (s); 1639 cm^{-1} (vs); 1390 cm^{-1} (s); 927 cm^{-1} (m); 914 cm^{-1} (ms); 737 cm^{-1} (m).

2.1.9. Preparation of $(H_3O)[Al_4(\mu\text{-}OH)(\mu\text{-}O)(hpdta)_2(O_2CNHC_3H_6NH_3)_2] \cdot 2(DMA) \cdot 13H_2O$ (**15**)

0.081 g (0.25 mmol) H_5hpdta and 0.188 g (0.5 mmol) $Al(NO_3)_3 \cdot 9H_2O$ were dissolved in 6 ml distilled water by slow addition of propylenediamine (ca. 0.1 ml) to a pH value of 8.6. Addition of 5 ml dimethylacetamide led to the formation of colourless plates within 2 days. Yield: 0.136 g (76% based on $Al(NO)_3 \cdot 9H_2O$). Elemental analysis, calculated for $Al_4C_{38}H_{84}N_{10}O_{35}$: C, 33.83; H, 6.28; N, 10.38; found, corresponds to the crystallographically determined formulation with the loss of five water molecules: C, 33.67; H, 6.45; N, 10.29%. IR data: 3427 cm^{-1} (s, br); 1652 cm^{-1} (vs); 1589 cm^{-1} (s); 1531 cm^{-1} (ms); 1385 cm^{-1} (vs); 926 cm^{-1} (m); 840 cm^{-1} (m).

2.2. X-ray crystallography

Details of the crystal structure analyses for the new structures presented here are summarised in Table 1. All structures except that of **2** were solved and refined using the SHELXTL 5.1 software package [6], with full-matrix least-squares refinement against F^2 for all data. In the case of **2**, the SHELXTL-PLUS 3.4 package [7] was used, and refinement was against F for observed ($F_o > 4\sigma(F_o)$) data.

In some of the structures, some solvent water molecules and/or organic cations were found to be disordered, but this could be modelled in a straightforward manner. In the case of **15**, the novel 3-ammoniocarbamate ligand was readily identified. The short (1.339(4) Å) bond between N(3) and C(12), the trigonal planar geometry around N(3), and the strong, almost linear hydrogen bond made by N(3)–H(3) to a carboxylate oxygen of an adjacent aggregate, all identified N(3) as an sp^2 nitrogen atom donating electron density from

Table 1
Crystal data

Compound	**1**	**2**	**3**	**4**	**11**	**13**	**14**	**15**
Formula	$C_{16}H_{26}Al_2N_4Na_2O_{19}$	$C_8H_{16}FeKN_2O_{11}$	$C_{16}H_{40}Fe_2K_4N_4O_{27}$	$C_8H_{20}Al_2N_2O_{14}$	$C_{11}H_{25}ClFe_2N_4O_{15}$	$C_{24}H_{55}Al_4N_6O_{29.5}$	$C_{50}H_{108}Fe_8N_{14}O_{56}$	$C_{38}H_{94}Al_4N_{10}O_{40}$
Formula weight	678.35	411.2	988.62	422.22	572.48	1007.66	2248.30	1439.15
Crystal system	Monoclinic	Orthorhombic	Monoclinic	Monoclinic	Monoclinic	Triclinic	Triclinic	Monoclinic
Space group	$P2_1/c$	$Pbcn$	$P2_1/c$	$C2/c$	$P2_1/n$	$P\bar{1}$	$P\bar{1}$	$P2_1/n$
a (Å)	15.261(5)	18.752(5)	11.120(3)	19.651(13)	7.4232(13)	14.383(2)	10.1510(10)	11.580(4)
b (Å)	16.696(5)	10.430(2)	17.147(3)	7.646(7)	13.8841(19)	14.426(2)	13.3392(19)	15.020(2)
c (Å)	10.312(3)	15.627(2)	9.529(2)	12.727(7)	20.775(4)	22.781(4)	16.557 (3)	19.050(3)
α (°)	90	90	90	90	90	100.87(2)	80.313(13)	90
β (°)	90.60(3)	90	105.81(2)	117.80(5)	92.753(14)	97.94(2)	85.142(11)	94.73(3)
γ (°)	90	90	90	90	90	114.15(2)	81.305(9)	90
U (Å^3)	2627.3(14)	3056.4(14)	1748.2(7)	1692(2)	2138.7(6)	4111.7(11)	2180.4(6)	3302.1(11)
Z	4	8	2	4	4	4	1	2
T (K)	293	293	293	293	293	200	200	200
$F(000)$	1400	1672	1016	880	1176	2116	1162	1528
D_{calc} (Mg m^{-3})	1.715	1.778	1.878	1.658	1.778	1.628	1.712	1.447
μ(Mo–K$_\alpha$) (mm^{-1})	0.241	1.313	1.412	0.250	1.557	0.224	1.406	0.176
Diffractometer	Siemens R3m/V	Siemens R3m/V	Siemens R3m/V	Siemens R3m/V	Siemens P4	Stoe IPDS	Rigaku AFC7R	Stoe IPDS
Crystal size (mm)	1.00 × 0.50 × 0.45	0.50 × 0.48 × 0.48	0.80 × 0.50 × 0.20	0.30 × 0.28 × 0.26	0.35 × 0.25 × 0.20	0.12 × 0.10 × 0.04	0.10 × 0.10 × 0.10	0.20 × 0.15 × 0.05
Data measured	4934	3232	3289	1461	4985	28566	8037	28016
Unique data	4654	2723	3090	1388	3673	14348	7673	6896
R_{int}	0.0110	0.004	0.1037	0.0806	0.0269	0.0492	0.0237	0.0537
Observed data: $I \geq 2\sigma(I)$	4224	2193	2422	952	3270	8397	5213	4743
Refinement against	F^2 (all data)	F [$I \geq 2\sigma(I)$]	F^2 (all data)	F^2 (all data)	F^2 (all data)	F^2 (all data)	F^2 (all data)	F^2 (all data)
Parameters/restraints	493/0	239/0	248/0	127/0	402/0	1221/24	635/27	488/0
wR_2, R_1 (all data)	0.0845, 0.0343	n.a., 0.0534	0.2929, 0.1158	0.3598, 0.1534	0.0777, 0.0355	0.1737, 0.1061	0.1497, 0.0881	0.1980, 0.0893
wR_2, R_1 [$I \geq 2\sigma(I)$]	0.0812, 0.0299	n.a., 0.0430	0.2715, 0.0937	0.3260, 0.1159	0.0723, 0.0355	0.1579, 0.0627	0.1309, 0.0445	0.1799, 0.0649
S (all data)	1.062	2.89	1.139	1.649	1.088	0.959	1.028	1.057
Mean/largest Δ/σ	0.000/0.001	0.002/0.021	0.000/0.000	0.000/0.001	0.000/0.001	0.000/0.000	0.000/0.002	0.000/0.002
Biggest difference peak/hole	0.243/−0.226	0.46/−0.53	2.596/−1.067	0.710/−0.931	0.402/−0.310	1.034/−0.568	2.357/−0.477	0.439/−0.352
CCDC reference	166903	166904	166905	166906	166907	166908	166909	166910

the *p*-orbital into the bridging carboxylate group; the hydrogen H(3) could be fully refined. Three hydrogens forming a tetrahedral geometry about the terminal atom of the chain could also be fully refined. They also each form strong hydrogen bonds to adjacent carboxylate oxygens, allowing N(4) to be identified as a terminal ammonium group. The central hydrogen was placed on the inversion centre between O(1) and O(1′), although it is possible that the hydrogen bond is not exactly symmetrical. O(1) and O(1′) are displaced by only 0.026(2) Å out of the Al_4 plane and are separated by only 2.363(3) Å, so that the possible alternative formulation with an $Al_4(OH)_2$ core, with the O–H bonds sharply bent out of the Al_4 plane, seems unlikely. This is discussed further below.

3. Results and discussion

The structures of the aluminium complexes described here underline the similarities in the structural preferences and hydrolytic chemistry of the Al(III) and Fe(III) (h.s.) ions, but also reveal some interesting differences. Iron(III) complexes have been obtained using all three iminodiacetate-derived ligands and we refer to these here to demonstrate these similarities and differences.

3.1. Complexes formed with H_2ida

In the presence of excess ligand, the simple mononuclear structure $Na[Al(ida)_2]\cdot 1.5H_2O$ (**1**) results where two iminodiacetate ligands act as if they were independent halves of edta, coordinating facially with the two nitrogen donors from the two ligands in a *cis* conformation about the Al(III) centre (Fig. 2a). These features have also been observed around the Fe(III) centre in $K[Fe(ida)_2]\cdot 3H_2O$ (**2**), (Fig. 2b). An interesting further feature of the Al(III) crystal structure is the interaction of the complexes with the sodium counterions. Thus, the asymmetric unit contains two independent but structurally very similar $[Al(ida)_2]^-$ complexes which at first sight appear to be related by translational symmetry, but the presence of chains of sodium counterions disrupts this (Fig. 2c). In contrast to the situation found for Fe(III)/ida complexes, it was not possible to produce an oxo-bridged 2:1 (ligand to metal) species corresponding to $[\{Fe(ida)_2\}_2O]^{4-}$ (**3**) (Fig. 3). In fact, μ-oxo bridged Al(III) dimer complexes are something of a rarity and this might reflect a preference for hydroxide coordination in the case of Al(III). Thus we see that when the ligand to metal ratio is reduced to 1:1, the dinuclear complex $[Al_2(\mu\text{-}OH)_2(ida)]\cdot 2H_2O$ (**4**) can be isolated (Fig. 4). Such a species was not observed for the Fe(III) system and in general relatively few diol-bridged Fe(III) dimers have been reported. In fact, for equivalent conditions for the Fe(III) system, we found that the

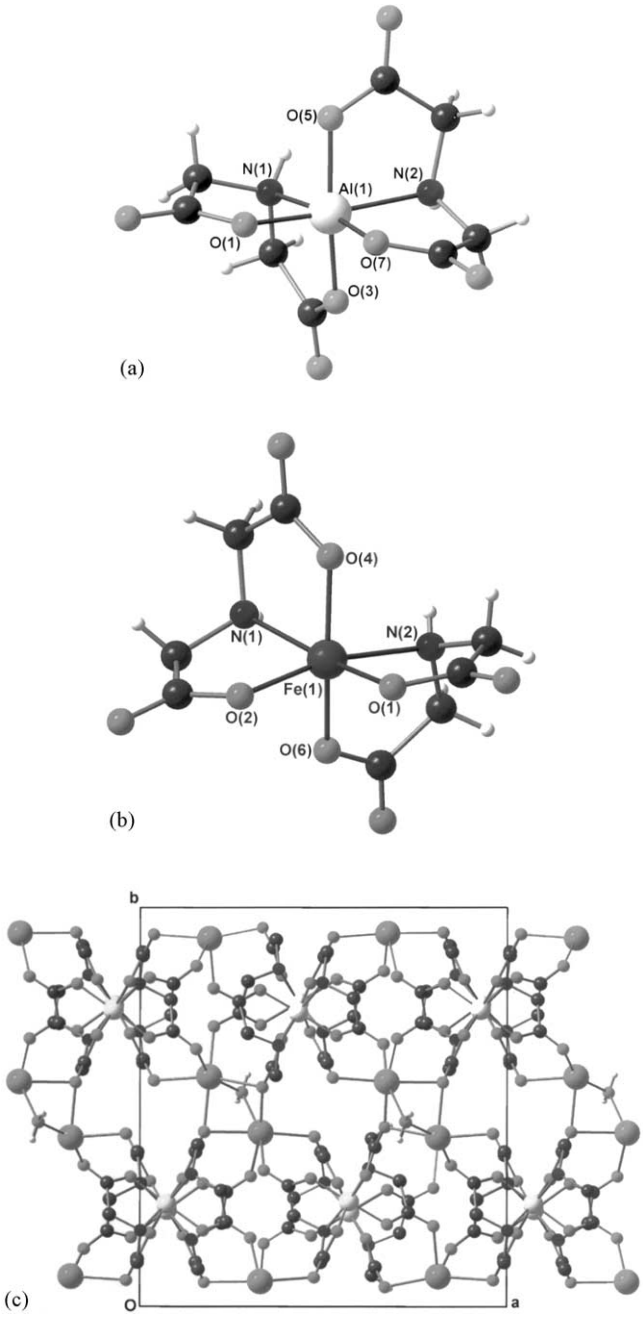

Fig. 2. (a) Structure of one of the $[Al(ida)_2]^-$ complex units in **1** (the other is isostructural). Al–N 2.042(2)–2.063(2) Å; Al–O 1.845(1)–1.879(1) Å. (b) Structure of the $[Fe(ida)_2]^-$ complex unit in **2**. Fe–N 2.148(3), 2.150(3) Å; Fe–O 1.970(3)–1.982(3) Å. (c) Crystal packing in **1**, viewed along *c* axis.

hexanuclear $[Fe_6(\mu_3\text{-}O)_2(\mu\text{-}OH)_6(ida)_6]^{4-}$ (**5**) species resulted [2]. A comparison of this cluster with the Al(III) dimer reveals the structural relationship between the two with both compounds being based on the unit $[M(ida)]^+$. If the Fe_6 core is represented as a combination of two Fe_3 subunits (see Fig. 5) it is possible to see how the dimer **4** could be converted into the Al_3 analogue of these Fe_3 subunits by replacing a proton from one of the μ-OH units with an $[M(ida)]^+$ unit.

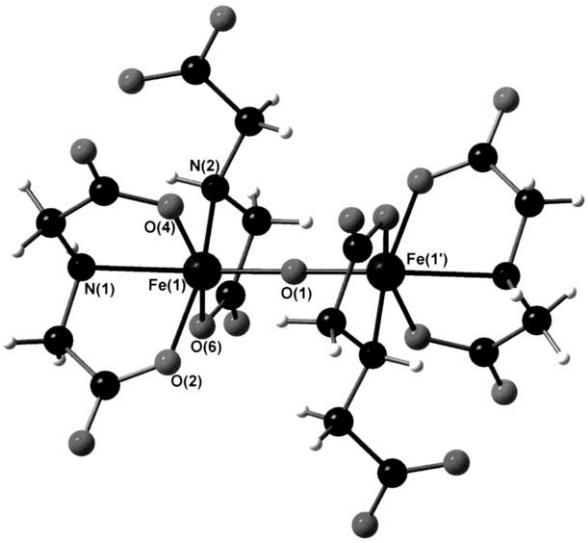

Fig. 3. Structure of $[Fe_2O(ida)_4]^{4-}$ anion in **3**. Fe(1)–O(1) 1.7956(13) Å; Fe(1)–O(1)–Fe(1′) 180°; Fe–N 2.181(8), 2.282(8) Å; Fe–O(carb) 2.031(7), 2.013(7), 2.078(7) Å.

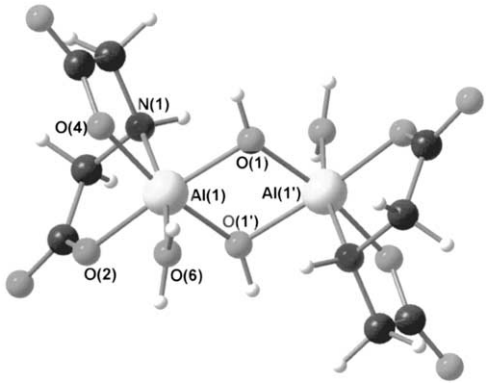

Fig. 4. Structure of $[Al_2(\mu\text{-}OH)_2(OH_2)_2(ida)_2]$ dimer in **4**. Al(1)–O(1) 1.849(6), Al(1′)–O(1) 1.847(6) Å; Al(1)–O(1)–Al(1′) 102.2(3)°; Al–N 2.083(6) Å; Al–O(carb) 1.873(7), 1.880(5) Å; Al–O(aq) 1.884(6) Å.

3.2. Complexes formed with H_3heidi

The replacement of the imine proton on H_2ida with a hydroxyethyl arm to give hydroxyethyliminodiacetic acid, H_3heidi, is a means of incorporating a dinucleating functionality into the ligand. With ligand to metal ratios of 1:1 alkoxide bridged dimers result for both Al(III) (**6**), and Fe(III) (**7**), of the general formula $[M(heidi)(H_2O)]_2$ (see Fig. 6) [3,4]. Of interest here is the ability of these two metal ions to promote the deprotonation of the alcohol function of the ligand which is a reflection of the general ability of these ions to activate O–H bonds, as seen in their normal hydrolysis reactions. Important also is the fact that the alkoxide arm links two metal centres together. This is useful in capturing hydrolysed oxy-hydroxide cores as seen for $[Al_{13}(\mu_3\text{-}OH)_6(\mu\text{-}OH)_{12}(heidi)_6(H_2O)_6]^{3+}$ (**8**) (Fig. 7) [3] and the Fe_{17} and Fe_{19} aggregates $[Fe_{17}(\mu_3\text{-}O)_4(\mu_3\text{-}OH)_6(\mu\text{-}OH)_{10}(heidi)_8(H_2O)_{12}]^{3+}$ (**9**) and $[Fe_{19}(\mu_3\text{-}O)_6(\mu_3\text{-}OH)_6(\mu\text{-}OH)_8(heidi)_{10}(H_2O)_{12}]^{+}$ (**10**) [4]. In all cases these contain a brucite derived $M(OH)_2$ core trapped in a shell of metal/ligand units. Again we observe a slightly different behaviour for the two metal ions in that the Al(III) structure only contains hydroxide bridges, but both iron(III) complexes have μ_3-oxo units as well. In addition, the aluminium(III) compound can be redissolved in water and retains its structure as seen from ^{27}Al-NMR studies [8], whereas the iron compounds can be interacted with water but decompose forming the dinuclear $[Fe(heidi)(H_2O)]_2$ (**7**) species with the excess iron forming a hydrolysed brown deposit [9].

3.3. Complexes formed with H_5hpdta

The ligand hydroxypropyldiaminotetracetic acid, H_5hpdta, can be regarded either as two iminodiacetic functionalities joined by a hydroxypropyl function or as a derivative of H_3heidi with a methyliminodiacetic acid arm attached to the β-carbon of the hydroxyethyl arm. It turns out that both Al(III) and Fe(III) display a rich hydrolytic chemistry in the presence of this ligand and we believe this owes much to the arrangement of the ligating groups which favour the initial formation of dinuclear species, $\{M_2(hpdta)(H_2O)_4\}^{+}$, presenting a water-rich face for further hydrolytic reactions. We have been able to crystallise this species for the Fe(III) system as a neutral molecule with one water ligand replaced by a chloride ligand, $[Fe_2(hpdta)(H_2O)_3Cl]$ (**11**) (Fig. 8), and in the light of the subsequent chemistry it is likely that this initial species is important in the Al(III) system as well. Thus we see a number of parallels in the compounds which form for both metals, although, again, there are some interesting differences in the finer details.

It is likely that for both metal ions a tetranuclear, essentially planar $\{M_4O(OH)(hpdta)_2(H_2O)_4\}^{-}$ species forms from the formal condensation of two dinuclear units with the loss of two water ligands and three protons. This arrangement has been structurally characterised for the Fe(III) system (compound **12**) [10]. It appears that this species is highly reactive, probably as a consequence of the terminal water ligands on the four metal centres. This core can be twisted to give a tetrahedral arrangement of the metal centres. For the Al(III) compound (**13**), the crystal structure analysis reveals that the core of this is formulated as $[Al_4(OH)_4(hpdta)_2]^{2-}$ (Fig. 9) which corresponds to the formal loss of two water ligands and one proton. This is slightly different from the iron case where the core corresponds to $[Fe_4O(OH)_3(hpdta)_2]^{3-}$ (**14**), i.e. with one oxide and three hydroxide bridges instead of the four hydroxide bridges observed for Al(III). In both cases this is a hydrolytically stable arrangement as all

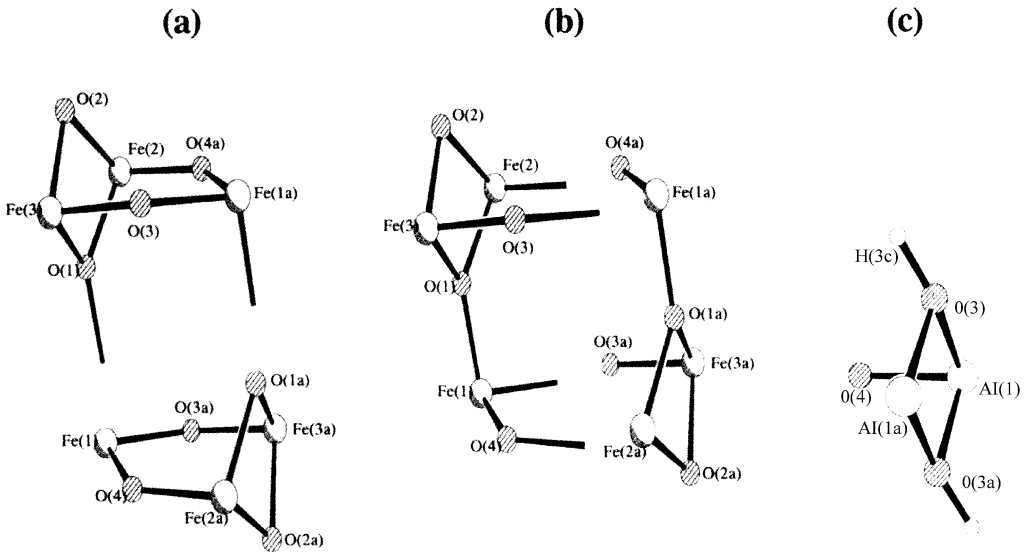

Fig. 5. Comparison of the core of the $[Fe_6(\mu_3\text{-}O)_2(\mu\text{-}OH)_6(ida)_6]^{4-}$ anion **5** (views a and b) and $[Al(ida)(OH)(H_2O)]_2$ (view c) **4** indicating how the dimer may represent a subunit of the hexanuclear compound.

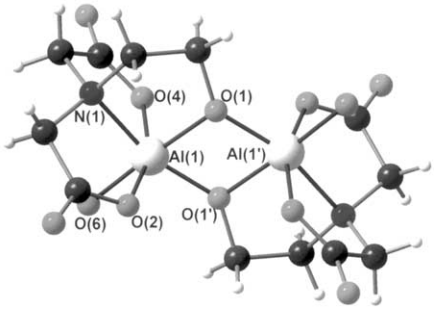

Fig. 6. Structure of $[Al_2(heidi)_2(OH_2)]$ in **6** (Ref. [3]). Al(1)–O(1) 1.898(6), Al(1′)–O(1) 1.797(8) Å; Al(1)–O(1)–Al(1′) 102.7(3)°. The analogous Fe_2 complex **7** is isostructural (Ref. [4]).

the water ligands have been lost or transformed into oxides and hydroxides. Similar arrangements have been observed for these metal ions with related dinucleating ligands [11].

Of more interest in terms of reactivity are the compounds which can be isolated for both systems where the hydrolytically active tetranuclear species $\{M_4O(OH)(hpdta)_2(H_2O)_4\}^-$ promotes new chemistry on substrates. We found that when we used propylenediamine as the hydrolysing base for the preparation of Al(III) aggregates a remarkably rapid reaction with aerial carbon dioxide took place resulting in the formation of crystals of $(H_3O)[Al_4(\mu\text{-}OH)(\mu\text{-}O)(hpdta)_2\text{-}(O_2CNHC_3H_6NH_3)_2]\cdot 2(DMA)\cdot 13H_2O$ (**15**), within 2 days in 76% yield, as verified from the powder pattern of the crystals not used in the single crystal structure determination. The core structure of **15** (Fig. 10) is made up of the tetranuclear arrangement of metal centres seen in the crystal structure analysis of the Fe(III) precursor analogue **12** with the places of the four water ligands occupied by two bridging carboxylate functions from

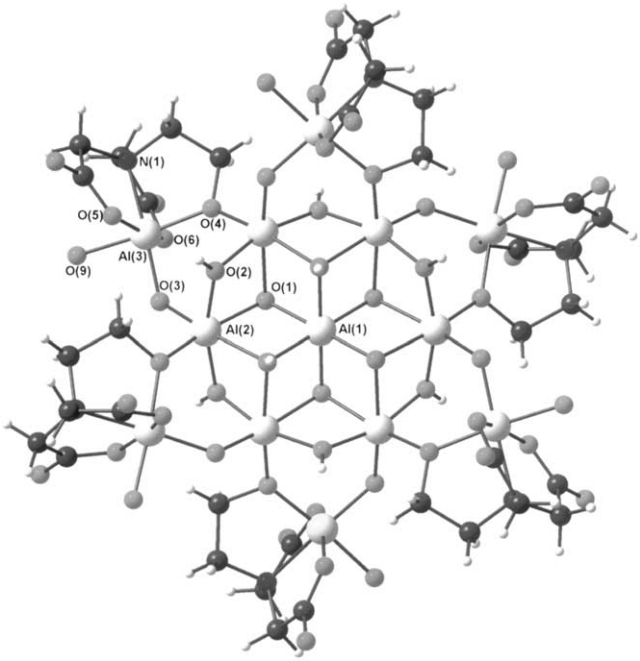

Fig. 7. Structure of $[Al_{13}(\mu_3\text{-}OH)_6(\mu\text{-}OH)_{12}(OH_2)_6(heidi)_6]^{3+}$ in **8** (Ref. [3]).

the carbamic acid formed between carbon dioxide and propylenediamine. These two ligands are actually in the zwitterionic form and the extra protons on the terminal amine group could be located in the crystal structure refinement. What is striking about this reaction is firstly the relative speed with which the crystals form, in turn suggesting that the compound must form quite rapidly and also the high yield of single crystals obtained. An analogous reaction has been observed for the Fe(III) system with propylenediamine and ethylenediamine, but the crystals form much more slowly and in much lower

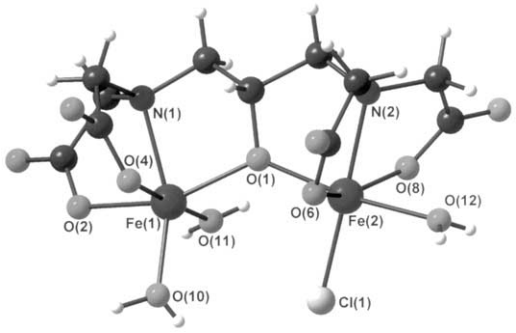

Fig. 8. Structure of $[Fe_2(hpdta)Cl(OH_2)_3]$ in **11**. Fe(1)–O(1) 2.070(2), Fe(2)–O(1) 2.036(2) Å; Fe(1)–O(1)–Fe(2) 133.24(9)°; Fe(2)–Cl(1) 2.254(1) Å; Fe–N 2.196(2), 2.209(2) Å; Fe–O(carb) 1.973(2)–2.077(2) Å; Fe–O(aq) 1.979(2)–2.172(2) Å.

yields along with the formation of various side products including iron hydroxide [10]. When aqueous solutions of propylenediamine with similar pH values to those used here are left to stand under analogous conditions, no significant reaction occurs, suggesting that the presence of the hydrolytically active aggregate is required for the activation of the carbon dioxide. A possible mechanism for the formation of the carbamic acid on the aggregate is given in Fig. 11. In this case we have given the possible steps for the activation and reaction of carbon dioxide and propylenediamine on one side of the core.

An interesting feature of the core structure observed for both the Al(III) and Fe(III) species is the unusual oxyhydroxide bridge in the centre of the core (see Fig. 10). We have written this as (O)(OH) in the chemical formula but the arrangement we assign corresponds to O···H···O. In the crystal structure analysis we can locate electron density equidistant from the two bridging oxygen atoms and cannot find any other electron density nearby. It should be noted that this electron density is located at a crystallographic inversion centre and the question arises as to whether this is an artefact. In fact, it is clear that we need to locate two positive charges in order to preserve charge neutrality. The protons on the carbamic acid ligand could all be satisfactorily located and the hydrogen bonding interactions indicate that the assignment of this ligand to the zwitterionic form is reasonable. In order to clarify the situation at the bridging oxygen centres we performed a bond valence sum calculation [12]. Not only did this effectively rule out the possibility of having two protons in a diol bridging type of arrangement since this would require O–H bond lengths of over 1.6 Å and the interactions from the carbamic acid ligands around the core make this highly unlikely, but it also proved to be in excellent agreement with the our assignment of a proton midway between the two oxygen atoms. The two oxygen atoms are only 2.36 Å apart which means that the O–H lengths should be 1.1–1.2 Å. The prediction

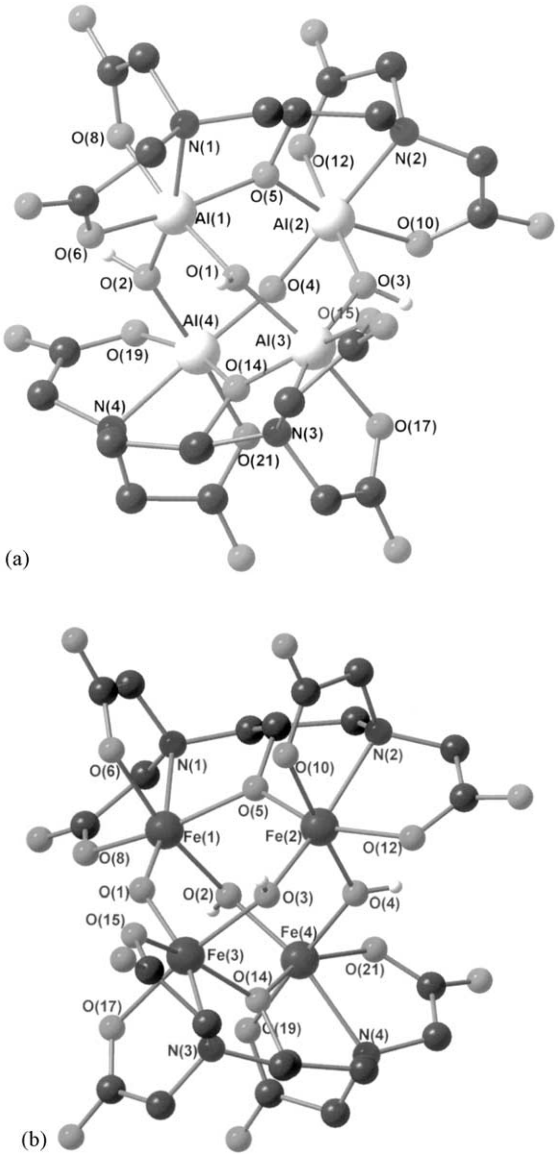

Fig. 9. (a) Structure of $[Al_4(\mu\text{-}OH)_4(hpdta)_2]^{2-}$ in **13** (the other Al_4 cluster in the asymmetric unit is isostructural). Al–O(H) 1.827(4)–1.928(4) Å; Al–O(H)–Al 130.5(2)–136.3(2)°; Al–O(alkoxy) 1.912(3)–1.936(3) Å; Al–O(alkoxy)–Al 129.6(2)–130.2(2)°. (b) Structure of $[Fe_4(\mu\text{-}O)(\mu\text{-}OH)_3(hpdta)_2]^{3-}$ in **14**. Fe(1)–O(1) 1.802(3), Fe(3)–O(1) 1.808(3) Å; Fe(1)–O(1)–Fe(3) 137.8(2)°; Fe–O(H) 1.921(3)–2.078(3) Å; Fe–O(H)–Fe 127.3(2)–128.8(2)°; Fe–O(alkoxy) 1.976(3)–2.016(3) Å, Fe–O(alkoxy)–Fe 126.5(2), 127.2(2)°.

from the bond valence sum calculation places a proton at ca. 1.2 Å. This seems, then, to be the reason for the very short O–O distance observed in the core. The remaining proton could be located satisfactorily in a hydrogen bonded situation involving a lattice water and three carboxylate groups to formally give a hydronium cation.

It is likely that the formation of a carbonate or bicarbonate ion on the core is an important step in the production of the carbamic acid ligand and we propose that this could occur through the hydration of CO_2 at the metal site. This is analogous to the situation in one

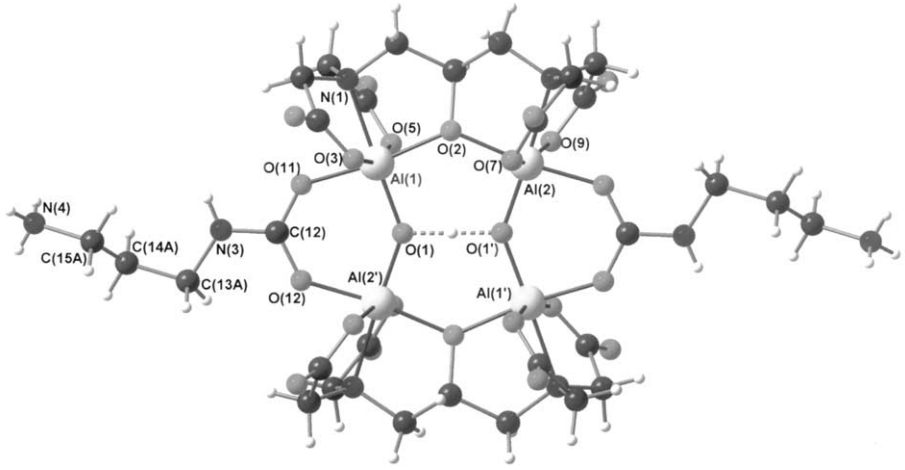

Fig. 10. Structure of $[Al_4(\mu\text{-OHO})(hpdta)_2(O_2CNHC_3H_6NH_3)_2]^-$ in **15**. For clarity, the minor disorder of the C_3H_6 unit in the carbamate and the central carbon of the hpdta ligand are omitted. Al(1)–O(1) 1.757(2), Al(2′)–O(1) 1.759(2), O(1)···O(1′) 2.363(3) Å; Al(1)–O(11) 1.890(2), Al(2′)–O(12) 1.917(2), O(11)–C(12) 1.277(3), O(12)–C(12) 1.265(4), C(12)–N(3) 1.339(4). N(3)–C(13A) 1.481(7) Å; Al(1)–O(1)–Al(2′) 139.8(1), Al(1)–O(2)–Al(2) 133.6(1)°; O(11)–C(12)–O(12) 126.2(2), O(11)–C(12)–N(3) 115.7(3), O(12)–C(12)–N(3) 118.0(2), C(12)–N(3)–C(13A) 122.0(4)°.

of the suggested mechanisms for the reaction of CO_2 with the Zn(II) centre in carbonic anhydrase [13]. This bicarbonate is then well placed to react with the amine group of the base allowing for the formation of the carbamic acid through elimination of a water molecule. This is, of course, the reverse reaction for the decomposition of a carbamic acid by hydrolysis. This new species, which is an example where a carbon–nitrogen bond has been formed via hydrolytic activation, is also of interest when considering the mechanism of urea decomposition in nickel urease which is believed to proceed *via* a carbamic acid intermediate formed as a bridging species between two nickel centres which are linked by a bridging hydroxide and possess terminal

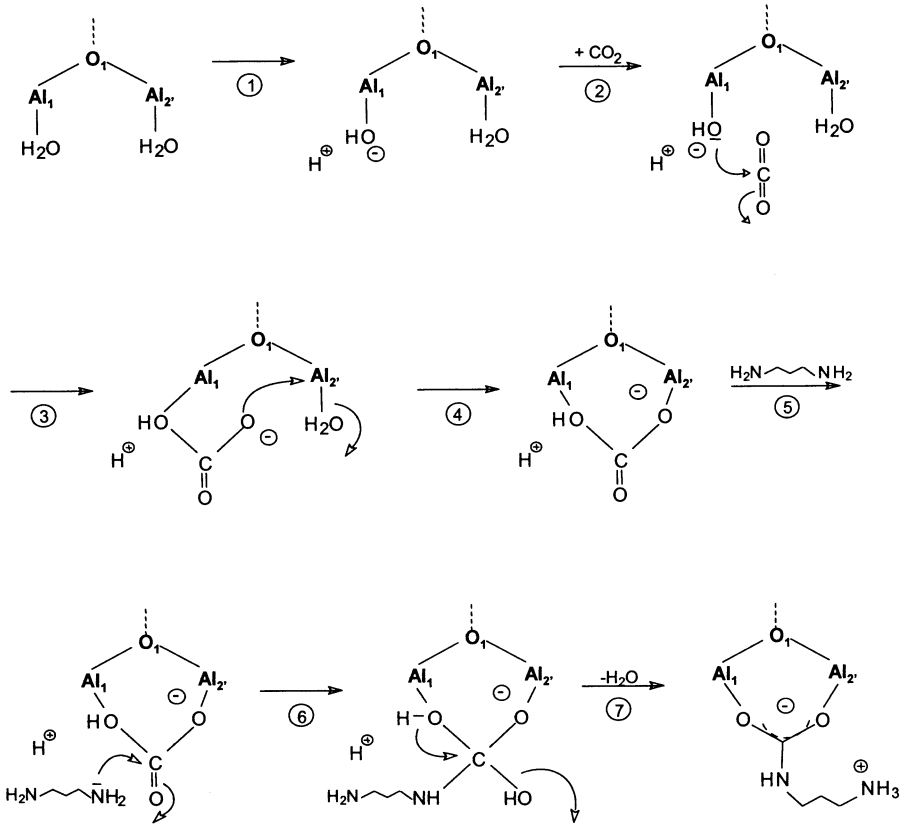

Fig. 11. Proposed reaction scheme leading to formation of the carbamate ligand in **15**.

water ligands in the resting state [14]. Overall, considering the relatively low concentration of carbon dioxide or, indeed, dissolved bicarbonate under these conditions it is striking how well the Al(III) aggregate fixes the CO_2. In fact, this compound proves to be rather stable and the carbamic acid ligand remains firmly fixed in

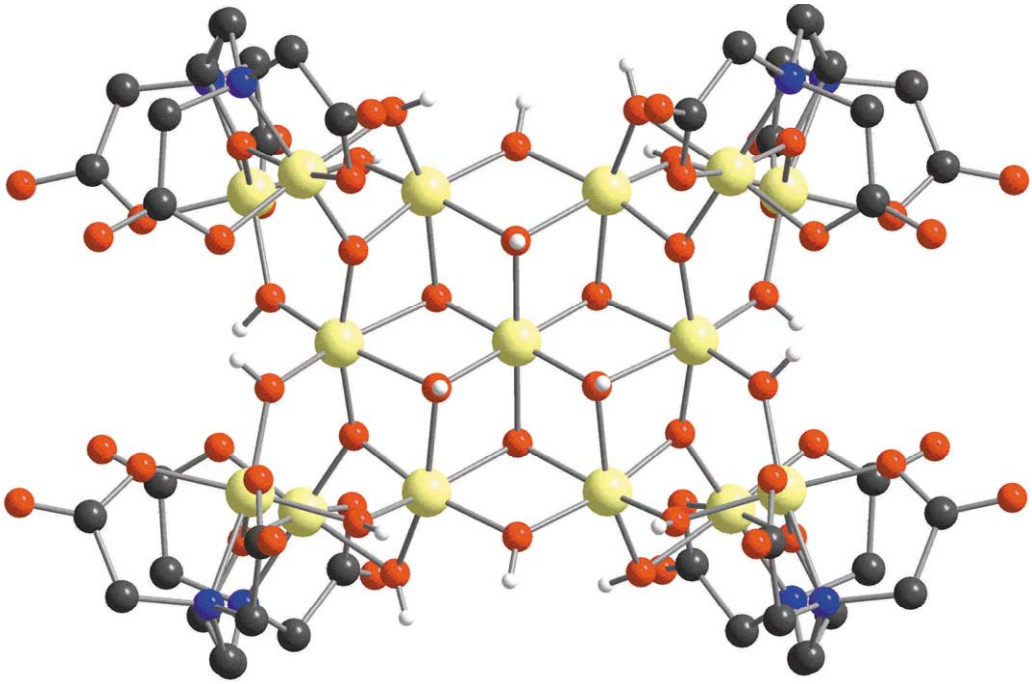

(a)

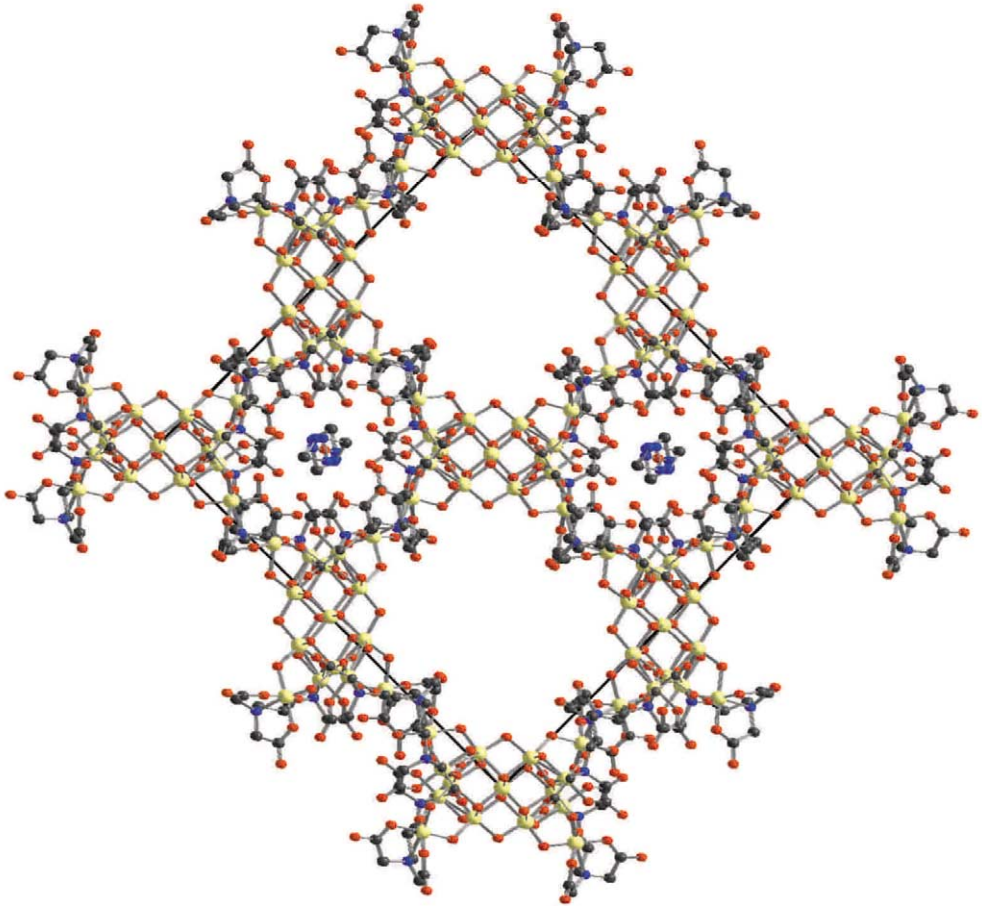

(b)

Fig. 12. (a) Structure of $[Al_{15}(\mu_3\text{-}O)_4(\mu_3\text{-}OH)_6(\mu\text{-}OH)_{14}(hpdta)_4]^{3-}$ in **16** and (b) zeotypic packing of Al_{15} aggregates (below) in **16** (Ref. [5]).

place so that although the compound sheds light on the hydrolytic activation of species by metal oxyhydroxy aggregates a further step where the carbamic acid is removed and the cycle continues cannot be realised. Perhaps, however, this suggests another means by which Al(III) can disrupt biochemical processes by becoming involved in reactions where stable intermediates instead of transient species are formed, thereby killing chemical or indeed catalytic transformations.

Finally, if the conditions for the preparation of the tetrahedral compound, $(enH_2)[Al_4(OH)_4(hpdta)_2]\cdot 7.5H_2O$ (**13**), are varied slightly, a further hydrolytic aggregate with 15 Al(III) centres can be isolated which forms either with ethylenediamine or piperazine as the hydrolysing base, the latter proving to give more suitable crystals for X-ray structure analysis, $(pipzH_2)(H_3O)[Al_{15}(\mu_3\text{-}O)_4(\mu_3\text{-}OH)_6(\mu\text{-}OH)_{14}(hpdta)_4]\cdot pipz\cdot 41H_2O$ (**16**) (Fig. 12) [5]. The structure has two important features. Firstly, the core of the aggregate corresponds to the core observed in compound **8**, having a brucite arrangement of the metal ions and hydroxides. Secondly, the cores pack together to give a zeotypic structure which is capable of containing and releasing solvent molecules held within large channels in the overall structure. These channels result from the outer ligand favouring quite strong interactions with templating cations arising from protonated base and water molecules which serve to hold the framework together and allow the crystals to be heated to 150 °C without losing their integrity. We were able to show the loss of solvent from the large channels and also noted the highly hygroscopic nature of the crystals indicating that solvent can be readily taken-up. Interestingly we have never observed the Fe(III) analogue of this compound. Instead a large variety of other aggregates form in the Fe(III) system [10]. These might also be present in the Al(III) system, or else this could be a case where the chemistries diverge with Al(III) producing more hydroxide-based aggregates and Fe(III) favouring the inclusion of oxide links as well.

4. Conclusions and outlook

The results presented here should help to further our understanding of the ways in which the Al^{3+} ion can interact with species present in aqueous environments. This is especially relevant these days as Al(III) is much more accessible to various chemical systems than it was before mankind developed means of obtaining the metal from its insoluble and unreactive ores and "released" it into the environment. The similarities between Al(III) and Fe(III) chemistries in aqueous systems suggest ways in which the Al^{3+} ion can gain access to various biological systems. The differences in the chemistries of Al(III) and iron in a general biological context may partly explain why Al(III) can be disruptive in such environments. In addition to the clear differences between Al(III) and, for example, Fe(II) there are more subtle differences in the hydrolytic behaviour of the two M(III) ions such as reactivity of hydrolytic aggregates and fine details of oxide and hydroxide preferences which could be important in finely balanced systems such as are found throughout biology. By using this comparative approach it should be possible to identify trends and patterns in Al(III) chemistry which indicate how Al(III) disrupts various biological processes and how it might be controlled.

5. Supplementary material

Crystallographic data (excluding structure factors) for the new structures presented in this paper have been deposited with the Cambridge Crystallographic Data Centre as supplementary publications. The CCDC deposition numbers are listed in Table 1. Copies of the data can be obtained, free of charge, on application to CCDC, 12 Union Road, Cambridge CB2 1EZ, UK, (fax: +44-1223-336-033; e-mail: deposit@ccdc.cam.ac.uk or www: http://www.ccdc.cam.ac.uk).

For convenience, the CCDC numbers available for previously published compounds mentioned in the text are as follows: **6** CCDC 166013, **8** CCDC 157371, **16** CCDC 163562. The structure of **5** has the CSD code (available through "QUEST" at Daresbury Laboratory, Daresbury, UK) refcode SUKXOL. Further details for the structures of **7** and **9** and **10** can be obtained from the Fachinformationszentrum Karlsruhe, Gesellschaft für Wissenschaftlich-technische Information mbH, D-76149, Eggenstein-Leopoldshafen 2, quoting the deposition number CSD-55936 and the details of Ref. [4].

References

[1] See for example, M. Nicolini, P.F. Zatta, B. Corain (Eds.), 1991. Aluminum in Chemistry, Biology and Medicine, Cortine International, Verona, Italy.
[2] C.J. Harding, R.K. Henderson, A.K. Powell, Angew. Chem. Int. Ed. Engl. 32 (1993) 570.
[3] S.L. Heath, P.A. Jordan, I.D. Johnson, G.R. Moore, A.K. Powell, M. Helliwell, J. Inorg. Biochem. 59 (1995) 785.
[4] S.L. Heath, A.K. Powell, Angew. Chem. Int. Ed. Engl. 31 (1992) 191.
[5] W. Schmitt, E. Baissa, A. Mandel, C.E. Anson, A.K. Powell, Angew. Chem. Int. Ed. Engl. 40 (2001) 3578.
[6] SHELXTL 5.1, Bruker AXS Inc., Madison, WI, 1999.
[7] SHELXTL-Plus 3.4, Siemens Analytical X-ray Instruments Inc., Madison, WI, 1989.
[8] P.A. Jordan, N.J. Clayden, S.L. Heath, G.R. Moore, A.K. Powell, A. Tapparo, Coord. Chem. Rev. 149 (1996) 281.
[9] J.C. Goodwin, R. Sessoli, D. Gatteschi, W. Wernsdorfer, A.L Barra, A.K. Powell, S.L. Heath, J. Chem. Soc. Dalton Trans. (2000) 1835.

[10] W. Schmitt, C.E. Anson, R. Sessoli, M. van Veen, A.K. Powell, J. Inorg. Biochem., in press.
[11] B.P. Murch, F.C. Bradley, P.D. Boyle, V. Papaefthymiou, L. Que, J. Am. Chem. Soc. 109 (1987) 7993.
[12] I.D. Brown, in: M. O'Keeffe, A. Navrotsky (Eds.), Structure and Bonding in Crystals, vol. II, Academic Press, New York, 1981, pp. 1–30.
[13] (a) K. Håkansson, M. Carlsson, L.A. Svensson, A. Liljas, J. Mol. Biol. 227 (1992) 1192;
(b) A.E. Eriksson, A. Liljas, Proteins Struct. Funct. Genetics 16 (1993) 29;
(c) J.E. Coleman, Annu. Rev. Biochem. 61 (1992) 897.
[14] (a) J.B. Sumner, J. Biol. Chem. 69 (1926) 435;
(b) H.L.T. Mobley, R.P. Hausinger, Microbiol. Rev. 53 (1989) 85;
(c) M.A. Pearson, L.O. Michel, R.P. Hausinger, P.A. Karplus, Biochemistry 36 (1997) 8164;
(d) A.M. Barrios, S.J. Lippard, J. Am. Chem. Soc. 121 (1999) 11751;
(e) B. Hommerich, H. Schwöppe, D. Volkmer, B. Krebs, Z. Anorg. Allg. Chem. 625 (1999) 75.